

LHCHWG-2024-002

February 21, 2024

LHC HIGGS WORKING GROUP^{*}
PUBLIC NOTE

Benchmark Lines and Planes for Higgs-to-Higgs Decays in the NMSSM

Conveners of the NMSSM Subgroup of WG3:

Ulrich Ellwanger^{1,†}, Margarete Mühlleitner^{2,‡}, Nikolaos Rompotis^{3,§}, Nausheen R. Shah^{4,¶}, Daniel Winterbottom^{5,||}

¹ *IJCLab, CNRS/IN2P3, University Paris-Saclay,
91405 Orsay, France*

² *Institute for Theoretical Physics, Karlsruhe Institute of Technology,
Wolfgang-Gaede-Str. 1, 76131 Karlsruhe, Germany*

³ *Oliver Lodge Laboratory, University of Liverpool,
Liverpool, L69 7ZE, United Kingdom*

⁴ *Department of Physics and Astronomy, Wayne State University,
Detroit, MI 48201, USA*

⁵ *Imperial College London, Physics Department, Blackett Laboratory,
Prince Consort Rd, London, SW7 2BW, United Kingdom*

^{*}<https://twiki.cern.ch/twiki/bin/view/LHCPhysics/LHCHWG>

[†]ulrich.ellwanger@ijclab.in2p3.fr

[‡]margarete.muehlleitner@kit.edu

[§]nikolaos.rompotis@cern.ch

[¶]nausheen.shah@wayne.edu

^{||}daniel.winterbottom@cern.ch

Abstract

A number of benchmark scenarios for NMSSM Higgs boson searches via Higgs-to-Higgs decays at the LHC have been proposed by the NMSSM Subgroup of the LHC HWG3. Some of them are already in use by the ATLAS and CMS collaborations for the interpretation of their results from Run 2. In this document we summarize the theory setup, the underlying procedures and reproduce the benchmark scenarios in table form.

1 The Higgs Sector of the NMSSM

The Next-to-Minimal Supersymmetric Standard Model (NMSSM) [1, 2] solves the μ -problem of the Minimal Supersymmetric Standard Model (MSSM) [3] since the supersymmetric mass term of the Higgs doublets is replaced by the vacuum expectation value (vev) of an extra gauge singlet scalar. This vev is naturally of the order of the supersymmetry breaking scale, somewhat larger than the electroweak scale. The neutral Higgs sector of the NMSSM consists of three complex scalars H_u^0 , H_d^0 and S where H_u^0 and H_d^0 are members of SU(2) doublets and S is a gauge singlet [1, 2]. Their self couplings originate from terms

$$W = \lambda \mathcal{H}_u \mathcal{H}_d \mathcal{S} + \frac{\kappa}{3} \mathcal{S}^3 + \dots \quad (1)$$

in the superpotential W in terms of superfields \mathcal{H} and \mathcal{S} , and from trilinear soft supersymmetry breaking terms

$$(\lambda A_\lambda H_u H_d S + \frac{\kappa}{3} A_\kappa S^3) + \text{h.c.} \quad (2)$$

Contributions from D -terms are relatively small. For the phenomenological analysis of this model, the self couplings have to be expressed in terms of physical states. To this end the weak eigenstates H_u^0 , H_d^0 and S have to be expanded around their vacuum expectation values v_u , v_d and v_s . The mass matrices have to be diagonalized, and in the CP-conserving case three neutral CP-even scalars and two neutral CP-odd scalars are obtained (after elimination of the Goldstone bosons). General expressions for these mass matrices including the dominant radiative corrections are given in Ref. [2].

A first approximation to the physical states is obtained in the so-called Higgs basis where singlet-doublet mixing is neglected and the CP-even doublets are rotated by the same angle as the CP-odd sector. Resulting approximate expressions for the physical masses and trilinear couplings among the physical states are given in Refs. [4, 5]; these allow us to understand orders of magnitude and hierarchies among the trilinear couplings.

The three CP-even scalars are denoted by H_1 , H_2 and H_3 , which are ordered in mass. The role of the observed SM-like Higgs scalar H_{SM} near 125 GeV is played by H_1 or H_2 depending on whether the mostly singlet-like scalar H_S is lighter or heavier than 125 GeV. The heaviest scalar H_3 is mostly MSSM-like, i.e. nearly degenerate with a CP-odd scalar (typically A_2 , with A_1 mostly singlet-like) and a charged Higgs scalar. The processes considered are of the form $ggF \rightarrow H_3 \rightarrow H_{SM} + H_S$ and $ggF \rightarrow A_2 \rightarrow H_{SM} + A_1$ for various decays of H_{SM} and H_S , and focusing on $A_1 \rightarrow \gamma\gamma$. The latter loop induced branching fraction can be particularly large once tree level couplings of A_1 to quarks and leptons are suppressed.

The cross sections times branching fractions (Xsect \times BRs) are computed, including radiative corrections to masses [6] and trilinear couplings [7–9], using the code **NMSSMTools** [10], and for some cases **NMSSMCALC** [11]. In addition to the NMSSM-specific parameters (λ , κ , A_λ and A_κ) these radiative corrections depend on Yukawa and gauge couplings, and on soft supersymmetry breaking squark, slepton, electroweak gaugino and gluino masses. In **NMSSMTools**, the H_3/A_2 Higgs production cross sections via ggF at $\sqrt{s} = 13$ TeV are taken from the TWiki web page [12] (update in CERN Report4 2016) multiplied by the squared reduced couplings of H_3 or A_2 to top quarks.

For a given set of masses of the two involved beyond-the-SM (BSM) Higgs bosons (one MSSM-like and one singlet-like), the Xsect \times BRs are maximized respecting constraints from previous searches for Higgs bosons, constraints from the properties of H_{SM} (couplings and mass, where we allow for a 3 GeV theory uncertainty), and constraints from b -physics and dark matter detection experiments. Hence regions of the

NMSSM parameter space can be identified where searches have the sensitivity to probe the presence of the two involved BSM Higgs bosons. However, this procedure does not allow us to exclude a given set of masses of these Higgs bosons since the Xsect \times BRs depends on additional parameters of the NMSSM.

Constraints from dark matter detection experiments are relevant since the dark matter relic density and detection cross section depend on the same NMSSM parameters as the Higgs sector. All these constraints are implemented in the code **NMSSMTools** [10] coupled to **MicrOmegas** [13]. Clearly, constraints from searches for BSM Higgs bosons and dark matter detection experiments are time dependent. Therefore we indicate for each benchmark plane which version of **NMSSMTools** has been used. The constraints applied in each version and the associated references can be found on the History tab of the **NMSSMTools** web page [14].

Further benchmark points or planes including Higgs pair production in the NMSSM can be found in Refs. [4, 5, 15–27].

2 Benchmark Planes

2.1 $b\bar{b}b\bar{b}$, $b\bar{b}\tau\tau$, $b\bar{b}\gamma\gamma$

Figure 1 shows the Xsect \times BRs for the processes $ggF \rightarrow H_3 \rightarrow (H_{SM} \rightarrow b\bar{b}/\tau\tau) + (H_S \rightarrow \tau\tau/b\bar{b})$, and $ggF \rightarrow A_2 \rightarrow (H_{SM} \rightarrow b\bar{b}) + (A_1 \rightarrow \gamma\gamma)$ as function of M_{H_3} or M_{A_2} , for $M_{H_S}, M_{A_1} \sim 100$ GeV. The corresponding numbers are given in Table 1 in the Appendix. The maximally possible Xsect \times BRs for $A_1 + H_{SM} \rightarrow \gamma\gamma + b\bar{b}$ can be relatively large since the BR($A_1 \rightarrow \gamma\gamma$) can be as large as $\sim 90\%$.

In Table 2 in the Appendix we show benchmark points for $ggF \rightarrow H_3 \rightarrow (H_{SM} \rightarrow \gamma\gamma) + (H_S \rightarrow b\bar{b})$ produced using **NMSSMTools_5.6.1**. However, constraints from $H/A \rightarrow Z+A/H$ by CMS [28] or ATLAS [29] and from $H/A \rightarrow H_{SM} + H/A$ by CMS [31] are switched off in order to allow comparisons of limits on Xsect \times BRs for $(H_{SM} \rightarrow \gamma\gamma) + (H_S \rightarrow b\bar{b})$ obtained by CMS in Ref. [30]. These benchmark points have been used in Ref [30].

2.2 $\tau\tau b\bar{b}$

In Table 3 in the Appendix we show maximally possible Xsect \times BRs for the processes $ggF \rightarrow H_3 \rightarrow (H_{SM} \rightarrow \tau\tau) + (H_S \rightarrow b\bar{b})$ for $400\text{GeV} \leq M_{H_3} \leq 600\text{GeV}$, $150\text{GeV} \leq M_{H_S} \leq 300\text{GeV}$ produced with **NMSSMTools_5.5.0**. These points were used to produce the 2D exclusion region in the CMS publication Ref. [31].

2.3 $b\bar{b}b\bar{b}/b\bar{b}\tau\tau$

In Table 4 in the Appendix we show maximally possible Xsect \times BRs for the processes $ggF \rightarrow H_3 \rightarrow (H_{SM} \rightarrow b\bar{b}/\tau\tau) + (H_S \rightarrow b\bar{b})$ for $900\text{GeV} \leq M_{H_3} \leq 3000\text{GeV}$, $62\text{GeV} \leq M_{H_S} \leq 600\text{GeV}$ produced with **NMSSMTools_5.6.1**. These points were used to produce the 2D exclusion region in the CMS publication Ref. [32].

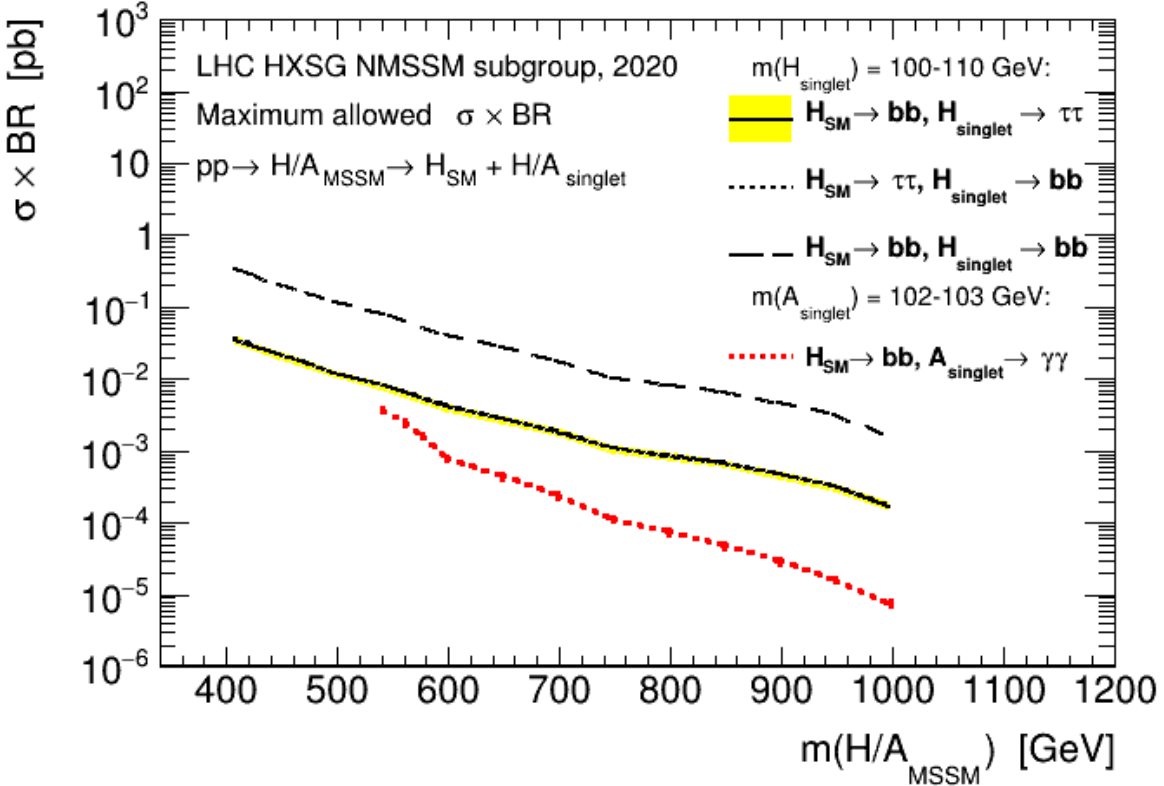


Figure 1: The lines correspond to the maximum cross-section times branching ratio allowed in the (real) NMSSM after experimental constraints from Higgs boson measurements, searches for supersymmetry, B-meson physics and dark matter detection as implemented in the used codes `NMSSMTools_5.5.0` [10] and `NMSSMCALC` [11]. The numbers are given in Table 1 in the Appendix.

2.4 $\tau\tau\gamma\gamma$

Table 5 in the Appendix lists maximally possible Xsect×BRs for the processes $ggF \rightarrow A_2 \rightarrow (H_{SM} \rightarrow \tau\tau) + (A_1 \rightarrow \gamma\gamma)$ produced with `NMSSMTools_5.5.0`.

2.5 $\tau\tau WW/ZZ$

Table 6 in the Appendix lists maximally possible Xsect×BRs for the processes $ggF \rightarrow H_3 \rightarrow (H_{SM} \rightarrow \tau\tau) + (H_S \rightarrow WW \text{ or } ZZ)$ produced with `NMSSMTools_6.0.0`. These points were used to produce the 2D exclusion region in the ATLAS publication Ref. [33].

Appendix

Table 1: Xsect \times BRs for the processes $ggF \rightarrow H_3 \rightarrow (H_{SM} \rightarrow b\bar{b}/\tau\tau) + (H_S \rightarrow \tau\tau/b\bar{b})$, and $ggF \rightarrow A_2 \rightarrow (H_{SM} \rightarrow b\bar{b}) + (A_1 \rightarrow \gamma\gamma)$ as function of M_{H_3} or M_{A_2} , for $M_{H_S}, M_{A_1} \sim 100$ GeV. The Xsect \times BRs for $H_3 \rightarrow (H_{SM} \rightarrow b\bar{b}) + (H_S \rightarrow b\bar{b})$ and for $(A_1 + H_{SM}) \rightarrow (\gamma\gamma + b\bar{b})$ in the format xx/yy denote Xsect \times BRs obtained by NMSSMTools_5.5.0 [10] or NMSSMCALC [11] respectively (not all mass combinations for $b\bar{b}b\bar{b}$ were obtained by NMSSMCALC). The Xsect \times BRs for $H_3 \rightarrow (H_{SM} \rightarrow b\bar{b}/\tau\tau) + (H_S \rightarrow \tau\tau/b\bar{b})$ in the format xx/yy denote Xsect \times BRs for $H_3 \rightarrow (H_{SM} \rightarrow \tau\tau) + (H_S \rightarrow b\bar{b})$ or $H_3 \rightarrow (H_{SM} \rightarrow b\bar{b}) + (H_S \rightarrow \tau\tau)$ respectively, both obtained by NMSSMTools_5.5.0. All Xsect \times BRs are given in pb.

M_{H_3}	Xsect \times BR for $b\bar{b}b\bar{b}$	Xsect \times BR for $b\bar{b}\tau\tau/\tau\tau b\bar{b}$	M_{A_2}	Xsect \times BR for $b\bar{b}\gamma\gamma$
408	$3.44 \cdot 10^{-1}/3.86 \cdot 10^{-1}$	$3.67 \cdot 10^{-2}/3.54 \cdot 10^{-2}$	540	$3.79 \cdot 10^{-3}$
422	$2.85 \cdot 10^{-1}/3.22 \cdot 10^{-1}$	$3.04 \cdot 10^{-2}/2.92 \cdot 10^{-2}$	560	$2.52 \cdot 10^{-3}$
447	$2.09 \cdot 10^{-1}/2.35 \cdot 10^{-1}$	$2.23 \cdot 10^{-2}/2.15 \cdot 10^{-2}$	577	$1.63 \cdot 10^{-3}$
472	$1.57 \cdot 10^{-1}$	$1.68 \cdot 10^{-2}/1.63 \cdot 10^{-2}$	599	$7.95 \cdot 10^{-4}$
497	$1.15 \cdot 10^{-1}$	$1.23 \cdot 10^{-2}/1.20 \cdot 10^{-2}$	648	$4.46 \cdot 10^{-4}$
547	$7.30 \cdot 10^{-2}/7.14 \cdot 10^{-2}$	$7.79 \cdot 10^{-3}/7.49 \cdot 10^{-3}$	698	$2.41 \cdot 10^{-4}$
597	$4.02 \cdot 10^{-2}$	$4.29 \cdot 10^{-3}/4.14 \cdot 10^{-3}$	748	$1.14 \cdot 10^{-4}$
647	$2.72 \cdot 10^{-2}/2.63 \cdot 10^{-2}$	$2.90 \cdot 10^{-3}/2.80 \cdot 10^{-3}$	798	$7.48 \cdot 10^{-5}$
697	$1.79 \cdot 10^{-2}$	$1.91 \cdot 10^{-3}/1.86 \cdot 10^{-3}$	848	$4.85 \cdot 10^{-5}$
747	$1.03 \cdot 10^{-2}$	$1.10 \cdot 10^{-3}/1.07 \cdot 10^{-3}$	898	$2.93 \cdot 10^{-5}$
797	$8.23 \cdot 10^{-3}/7.19 \cdot 10^{-3}$	$8.79 \cdot 10^{-4}/8.53 \cdot 10^{-4}$	948	$1.63 \cdot 10^{-5}$
847	$6.47 \cdot 10^{-3}/5.29 \cdot 10^{-3}$	$6.90 \cdot 10^{-4}/6.67 \cdot 10^{-4}$	998	$7.56 \cdot 10^{-6}$
897	$4.59 \cdot 10^{-3}/3.56 \cdot 10^{-3}$	$4.89 \cdot 10^{-4}/4.74 \cdot 10^{-4}$	-	-
947	$3.11 \cdot 10^{-3}/2.50 \cdot 10^{-3}$	$3.31 \cdot 10^{-4}/3.21 \cdot 10^{-4}$	-	-
997	$1.64 \cdot 10^{-3}/1.83 \cdot 10^{-3}$	$1.74 \cdot 10^{-4}/1.69 \cdot 10^{-4}$	-	-

Table 2: Maximally possible Xsect \times BRs (in pb) at 13 TeV for $ggF \rightarrow H_3 \rightarrow (H_{SM} \rightarrow \gamma\gamma) + (H_S \rightarrow b\bar{b})$ produced using **NMSSMTools_5.6.1**. Constraints from $H/A \rightarrow Z + A/H$ by CMS [28] or ATLAS [29] and from $H/A \rightarrow H_{SM} + H/A$ by CMS [31] are switched off.

M_{H_3}	M_{H_S}	Xsect \times BR	M_{H_3}	M_{H_S}	Xsect \times BR	M_{H_3}	M_{H_S}	Xsect \times BR
410	90	$0.141 \cdot 10^{-2}$	409	100	$0.155 \cdot 10^{-2}$	400	150	$0.923 \cdot 10^{-3}$
400	200	$0.109 \cdot 10^{-2}$	400	250	$0.141 \cdot 10^{-4}$	500	90	$0.522 \cdot 10^{-3}$
500	100	$0.527 \cdot 10^{-3}$	500	150	$0.472 \cdot 10^{-3}$	500	200	$0.386 \cdot 10^{-3}$
500	250	$0.329 \cdot 10^{-3}$	500	300	$0.253 \cdot 10^{-3}$	600	90	$0.193 \cdot 10^{-3}$
600	100	$0.194 \cdot 10^{-3}$	600	150	$0.190 \cdot 10^{-3}$	600	200	$0.182 \cdot 10^{-3}$
600	250	$0.722 \cdot 10^{-4}$	600	300	$0.142 \cdot 10^{-3}$	600	400	$0.103 \cdot 10^{-4}$
700	90	$0.800 \cdot 10^{-4}$	700	100	$0.802 \cdot 10^{-4}$	700	150	$0.772 \cdot 10^{-4}$
700	200	$0.795 \cdot 10^{-4}$	700	250	$0.758 \cdot 10^{-4}$	700	300	$0.502 \cdot 10^{-4}$
700	400	$0.129 \cdot 10^{-4}$	700	500	$0.197 \cdot 10^{-5}$	800	90	$0.345 \cdot 10^{-4}$
800	100	$0.349 \cdot 10^{-4}$	800	150	$0.354 \cdot 10^{-4}$	800	200	$0.347 \cdot 10^{-4}$
800	250	$0.236 \cdot 10^{-4}$	800	300	$0.212 \cdot 10^{-4}$	800	400	$0.635 \cdot 10^{-5}$
800	500	$0.229 \cdot 10^{-5}$	800	600	$0.463 \cdot 10^{-6}$	900	90	$0.162 \cdot 10^{-4}$
900	100	$0.160 \cdot 10^{-4}$	900	150	$0.153 \cdot 10^{-4}$	900	200	$0.154 \cdot 10^{-4}$
900	250	$0.130 \cdot 10^{-4}$	900	300	$0.126 \cdot 10^{-4}$	900	400	$0.216 \cdot 10^{-5}$
900	500	$0.117 \cdot 10^{-5}$	900	600	$0.629 \cdot 10^{-6}$	900	700	$0.311 \cdot 10^{-7}$
1000	90	$0.749 \cdot 10^{-5}$	1000	100	$0.742 \cdot 10^{-5}$	1000	150	$0.756 \cdot 10^{-5}$
1000	200	$0.788 \cdot 10^{-5}$	1000	250	$0.559 \cdot 10^{-5}$	1000	300	$0.507 \cdot 10^{-5}$
1000	400	$0.125 \cdot 10^{-5}$	1000	500	$0.615 \cdot 10^{-6}$	1000	600	$0.471 \cdot 10^{-6}$
1000	700	$0.220 \cdot 10^{-6}$	1000	800	$0.236 \cdot 10^{-7}$	-	-	-

Table 3: Maximally possible Xsect \times BRs (in pb) at 13 TeV for $ggF \rightarrow H_3 \rightarrow (H_{SM} \rightarrow \tau\tau) + (H_S \rightarrow b\bar{b})$ produced with **NMSSMTools_5.5.0**.

M_{H_3}	M_{H_S}	Xsect \times BR	M_{H_3}	M_{H_S}	Xsect \times BR
400	190	$0.2870 \cdot 10^{-1}$	400	250	$0.8118 \cdot 10^{-2}$
450	190	$0.2278 \cdot 10^{-1}$	450	250	$0.1722 \cdot 10^{-1}$
500	250	$0.1217 \cdot 10^{-1}$	500	300	$0.7850 \cdot 10^{-2}$
550	190	$0.9352 \cdot 10^{-2}$	550	250	$0.7609 \cdot 10^{-2}$
600	150	$0.4257 \cdot 10^{-2}$	600	170	$0.5056 \cdot 10^{-2}$

Table 4: Maximally possible Xsect \times BRs (in pb) at 13 TeV for $ggF \rightarrow H_3 \rightarrow (H_{SM} \rightarrow b\bar{b}) + (H_S \rightarrow b\bar{b})$ and $ggF \rightarrow H_3 \rightarrow (H_{SM} \rightarrow \tau\tau) + (H_S \rightarrow b\bar{b})$ produced with NMSSMTools_5.6.1.

M_{H_3}	M_{H_S}	$H_{SM} \rightarrow b\bar{b}$	$H_{SM} \rightarrow \tau\tau$	M_{H_3}	M_{H_S}	$H_{SM} \rightarrow b\bar{b}$	$H_{SM} \rightarrow \tau\tau$
900	62	$0.409 \cdot 10^{-2}$	$0.436 \cdot 10^{-3}$	900	80	$0.408 \cdot 10^{-2}$	$0.434 \cdot 10^{-3}$
900	100	$0.405 \cdot 10^{-2}$	$0.431 \cdot 10^{-3}$	900	120	$0.412 \cdot 10^{-2}$	$0.438 \cdot 10^{-3}$
900	130	$0.415 \cdot 10^{-2}$	$0.441 \cdot 10^{-3}$	900	150	$0.412 \cdot 10^{-2}$	$0.447 \cdot 10^{-3}$
900	200	$0.430 \cdot 10^{-2}$	$0.458 \cdot 10^{-3}$	900	300	$0.340 \cdot 10^{-2}$	$0.361 \cdot 10^{-3}$
900	400	$0.593 \cdot 10^{-3}$	$0.630 \cdot 10^{-4}$	900	500	$0.330 \cdot 10^{-3}$	$0.351 \cdot 10^{-4}$
900	600	$0.179 \cdot 10^{-3}$	$0.190 \cdot 10^{-4}$	1000	62	$0.191 \cdot 10^{-2}$	$0.203 \cdot 10^{-3}$
1000	80	$0.191 \cdot 10^{-2}$	$0.203 \cdot 10^{-3}$	1000	100	$0.189 \cdot 10^{-2}$	$0.201 \cdot 10^{-3}$
1000	120	$0.193 \cdot 10^{-2}$	$0.205 \cdot 10^{-3}$	1000	130	$0.201 \cdot 10^{-2}$	$0.214 \cdot 10^{-3}$
1000	150	$0.206 \cdot 10^{-2}$	$0.219 \cdot 10^{-3}$	1000	200	$0.217 \cdot 10^{-2}$	$0.231 \cdot 10^{-3}$
1000	300	$0.134 \cdot 10^{-2}$	$0.143 \cdot 10^{-3}$	1000	400	$0.341 \cdot 10^{-3}$	$0.362 \cdot 10^{-4}$
1000	500	$0.171 \cdot 10^{-3}$	$0.182 \cdot 10^{-4}$	1000	600	$0.131 \cdot 10^{-3}$	$0.139 \cdot 10^{-4}$
1200	62	$0.516 \cdot 10^{-3}$	$0.550 \cdot 10^{-4}$	1200	80	$0.513 \cdot 10^{-3}$	$0.546 \cdot 10^{-4}$
1200	100	$0.504 \cdot 10^{-3}$	$0.536 \cdot 10^{-4}$	1200	150	$0.492 \cdot 10^{-3}$	$0.527 \cdot 10^{-4}$
1200	200	$0.547 \cdot 10^{-3}$	$0.582 \cdot 10^{-4}$	1200	300	$0.447 \cdot 10^{-3}$	$0.475 \cdot 10^{-4}$
1200	400	$0.110 \cdot 10^{-3}$	$0.117 \cdot 10^{-4}$	1200	500	$0.564 \cdot 10^{-4}$	$0.600 \cdot 10^{-5}$
1200	600	$0.422 \cdot 10^{-4}$	$0.449 \cdot 10^{-5}$	1400	62	$0.161 \cdot 10^{-3}$	$0.171 \cdot 10^{-4}$
1400	80	$0.168 \cdot 10^{-3}$	$0.179 \cdot 10^{-4}$	1400	100	$0.154 \cdot 10^{-3}$	$0.165 \cdot 10^{-4}$
1400	120	$0.153 \cdot 10^{-3}$	$0.163 \cdot 10^{-4}$	1400	130	$0.152 \cdot 10^{-3}$	$0.163 \cdot 10^{-4}$
1400	150	$0.156 \cdot 10^{-3}$	$0.166 \cdot 10^{-4}$	1400	200	$0.140 \cdot 10^{-3}$	$0.149 \cdot 10^{-4}$
1400	300	$0.129 \cdot 10^{-3}$	$0.137 \cdot 10^{-4}$	1400	400	$0.410 \cdot 10^{-4}$	$0.436 \cdot 10^{-5}$
1400	500	$0.214 \cdot 10^{-4}$	$0.228 \cdot 10^{-5}$	1400	600	$0.161 \cdot 10^{-4}$	$0.171 \cdot 10^{-5}$
1600	62	$0.480 \cdot 10^{-4}$	$0.512 \cdot 10^{-5}$	1600	80	$0.473 \cdot 10^{-4}$	$0.504 \cdot 10^{-5}$
1600	100	$0.439 \cdot 10^{-4}$	$0.467 \cdot 10^{-5}$	1600	150	$0.432 \cdot 10^{-4}$	$0.459 \cdot 10^{-5}$
1600	200	$0.448 \cdot 10^{-4}$	$0.477 \cdot 10^{-5}$	1600	300	$0.312 \cdot 10^{-4}$	$0.331 \cdot 10^{-5}$
1600	400	$0.128 \cdot 10^{-4}$	$0.136 \cdot 10^{-5}$	1600	500	$0.639 \cdot 10^{-5}$	$0.679 \cdot 10^{-6}$
1600	600	$0.469 \cdot 10^{-5}$	$0.499 \cdot 10^{-6}$	1800	62	$0.169 \cdot 10^{-4}$	$0.180 \cdot 10^{-5}$
1800	80	$0.168 \cdot 10^{-4}$	$0.179 \cdot 10^{-5}$	1800	100	$0.165 \cdot 10^{-4}$	$0.176 \cdot 10^{-5}$
1800	150	$0.150 \cdot 10^{-4}$	$0.160 \cdot 10^{-5}$	1800	200	$0.154 \cdot 10^{-4}$	$0.164 \cdot 10^{-5}$
1800	300	$0.820 \cdot 10^{-5}$	$0.872 \cdot 10^{-6}$	1800	400	$0.469 \cdot 10^{-5}$	$0.498 \cdot 10^{-6}$
1800	500	$0.254 \cdot 10^{-5}$	$0.270 \cdot 10^{-6}$	1800	600	$0.187 \cdot 10^{-5}$	$0.199 \cdot 10^{-6}$
2000	62	$0.661 \cdot 10^{-5}$	$0.703 \cdot 10^{-6}$	2000	80	$0.659 \cdot 10^{-5}$	$0.700 \cdot 10^{-6}$
2000	100	$0.662 \cdot 10^{-5}$	$0.704 \cdot 10^{-6}$	2000	150	$0.653 \cdot 10^{-5}$	$0.695 \cdot 10^{-6}$
2000	200	$0.637 \cdot 10^{-5}$	$0.678 \cdot 10^{-6}$	2000	300	$0.283 \cdot 10^{-5}$	$0.301 \cdot 10^{-6}$
2000	400	$0.191 \cdot 10^{-5}$	$0.203 \cdot 10^{-6}$	2000	500	$0.123 \cdot 10^{-5}$	$0.130 \cdot 10^{-6}$
2000	600	$0.106 \cdot 10^{-5}$	$0.113 \cdot 10^{-6}$	2500	62	$0.555 \cdot 10^{-6}$	$0.591 \cdot 10^{-7}$
2500	80	$0.587 \cdot 10^{-6}$	$0.625 \cdot 10^{-7}$	2500	100	$0.594 \cdot 10^{-6}$	$0.632 \cdot 10^{-7}$
2500	150	$0.613 \cdot 10^{-6}$	$0.653 \cdot 10^{-7}$	2500	200	$0.664 \cdot 10^{-6}$	$0.707 \cdot 10^{-7}$
2500	300	$0.524 \cdot 10^{-6}$	$0.558 \cdot 10^{-7}$	2500	400	$0.384 \cdot 10^{-6}$	$0.408 \cdot 10^{-7}$
2500	500	$0.235 \cdot 10^{-6}$	$0.250 \cdot 10^{-7}$	2500	600	$0.179 \cdot 10^{-6}$	$0.190 \cdot 10^{-7}$
3000	150	$0.404 \cdot 10^{-7}$	$0.430 \cdot 10^{-8}$	3000	200	$0.238 \cdot 10^{-7}$	$0.254 \cdot 10^{-8}$

Table 5: Maximally possible Xsect \times BRs (in pb) at 13 TeV for $ggF \rightarrow A_2 \rightarrow (H_{SM} \rightarrow \tau\tau) + (A_1 \rightarrow \gamma\gamma)$ produced with NMSSMTools_5.5.0.

M_{A_2}	M_{A_1}	Xsect \times BR	M_{A_2}	M_{A_1}	Xsect \times BR
410	70	$0.408 \cdot 10^{-2}$	405	100	$0.885 \cdot 10^{-2}$
411	170	$0.524 \cdot 10^{-2}$	413	200	$0.406 \cdot 10^{-2}$
500	70	$0.916 \cdot 10^{-3}$	500	100	$0.162 \cdot 10^{-2}$
500	200	$0.126 \cdot 10^{-2}$	600	70	$0.214 \cdot 10^{-3}$
600	100	$0.365 \cdot 10^{-3}$	600	200	$0.370 \cdot 10^{-3}$
700	70	$0.668 \cdot 10^{-4}$	700	100	$0.110 \cdot 10^{-3}$
700	200	$0.118 \cdot 10^{-3}$	-	-	-

Table 6: Maximally possible Xsect \times BRs (in pb) at 13 TeV for $ggF \rightarrow H_3 \rightarrow (H_{SM} \rightarrow \tau\tau) + (H_S \rightarrow WW)$ and $ggF \rightarrow H_3 \rightarrow (H_{SM} \rightarrow \tau\tau) + (H_S \rightarrow ZZ)$ produced with NMSSMTools_6.0.0.

M_{H_3}	M_{H_S}	$H_S \rightarrow WW$	$H_S \rightarrow ZZ$	M_{H_3}	M_{H_S}	$H_S \rightarrow WW$	$H_S \rightarrow ZZ$
500	200	$0.809 \cdot 10^{-2}$	$0.278 \cdot 10^{-2}$	500	300	$0.420 \cdot 10^{-2}$	$0.186 \cdot 10^{-2}$
750	200	$0.118 \cdot 10^{-2}$	$0.405 \cdot 10^{-3}$	750	300	$0.587 \cdot 10^{-3}$	$0.261 \cdot 10^{-3}$
750	400	$0.379 \cdot 10^{-3}$	$0.176 \cdot 10^{-3}$	750	500	$0.208 \cdot 10^{-3}$	$0.994 \cdot 10^{-4}$
1000	200	$0.114 \cdot 10^{-3}$	$0.395 \cdot 10^{-4}$	1000	300	$0.100 \cdot 10^{-3}$	$0.444 \cdot 10^{-4}$
1000	400	$0.961 \cdot 10^{-4}$	$0.448 \cdot 10^{-4}$	1000	500	$0.105 \cdot 10^{-3}$	$0.501 \cdot 10^{-4}$
1250	200	$0.231 \cdot 10^{-4}$	$0.794 \cdot 10^{-5}$	1250	300	$0.232 \cdot 10^{-4}$	$0.103 \cdot 10^{-4}$
1250	400	$0.256 \cdot 10^{-4}$	$0.119 \cdot 10^{-4}$	1250	500	$0.257 \cdot 10^{-4}$	$0.123 \cdot 10^{-4}$
1500	200	$0.554 \cdot 10^{-5}$	$0.191 \cdot 10^{-5}$	1500	300	$0.546 \cdot 10^{-5}$	$0.243 \cdot 10^{-5}$
1500	400	$0.621 \cdot 10^{-5}$	$0.289 \cdot 10^{-5}$	1500	500	$0.652 \cdot 10^{-5}$	$0.311 \cdot 10^{-5}$

References

- [1] M. Maniatis, Int. J. Mod. Phys. A **25** (2010), 3505-3602 [arXiv:0906.0777 [hep-ph]].
- [2] U. Ellwanger, C. Hugonie and A. M. Teixeira, Phys. Rept. **496** (2010) 1 [arXiv:0910.1785 [hep-ph]].
- [3] J. E. Kim and H. P. Nilles, Phys. Lett. B **138** (1984), 150-154
- [4] M. Carena, H. E. Haber, I. Low, N. R. Shah and C. E. M. Wagner, Phys. Rev. D **93** (2016) no.3, 035013 [arXiv:1510.09137 [hep-ph]].
- [5] U. Ellwanger and C. Hugonie, Eur. Phys. J. C **82** (2022) no.5, 406 [arXiv:2203.05049 [hep-ph]].
- [6] P. Slavich, P. et al., Eur. Phys. J. C **81** (2021) 450 [arXiv:2012.15629].
- [7] M. Mühlleitner, D. T. Nhungh, J. Streicher, and K. Walz, JHEP **11** (2013) 181 [arXiv:1306.3926].
- [8] M. Mühlleitner, D. T. Nhungh, and H. Ziesche, JHEP **12** (2015) 034, [arXiv:1506.03321].
- [9] C. Borschensky, T. N. Dao, M. Gabelmann, M. Mühlleitner, and H. Rzezhak, Eur. Phys. J. C **83** (2023) 118, [arXiv:2210.02104].
- [10] U. Ellwanger, J. F. Gunion and C. Hugonie, JHEP **0502** (2005) 066, [hep-ph/0406215], and U. Ellwanger and C. Hugonie, Comput. Phys. Commun. **175** (2006) 290 [hep-ph/0508022].
<https://www.lupm.in2p3.fr/users/nmssm/index.html>
- [11] J. Baglio, R. Gröber, M. Mühlleitner, D. T. Nhungh, H. Rzezhak, M. Spira, J. Streicher and K. Walz, Comput. Phys. Commun. **185** (2014) no.12, 3372-3391 [arXiv:1312.4788 [hep-ph]].
<https://www.itp.kit.edu/maggie/NMSSMCALC/>
- [12] <https://twiki.cern.ch/twiki/bin/view/LHCPhysics/CERNYellowReportPageBSMAt13TeV>
- [13] G. Belanger, F. Boudjema, A. Pukhov and A. Semenov, Comput. Phys. Commun. **185** (2014), 960-985 [arXiv:1305.0237 [hep-ph]].
- [14] <https://www.lupm.in2p3.fr/users/nmssm/history.html>
- [15] S. F. King, M. Mühlleitner, and R. Nevezorov, Nucl. Phys. **B860** (2012) 207 [arXiv:1201.2671].
- [16] Z. Kang, J. Li, T. Li, D. Liu and J. Shu, Phys. Rev. D **88** (2013) no.1, 015006 [arXiv:1301.0453 [hep-ph]].
- [17] S. F. King, M. Mühlleitner, R. Nevezorov and K. Walz, Phys. Rev. D **90** (2014) no.9, 095014 [arXiv:1408.1120 [hep-ph]].
- [18] U. Ellwanger and M. Rodriguez-Vazquez, JHEP **02** (2016), 096 [arXiv:1512.04281 [hep-ph]].
- [19] R. Costa, M. Mühlleitner, M. O. P. Sampaio and R. Santos, JHEP **06** (2016), 034 [arXiv:1512.05355 [hep-ph]].

- [20] S. Baum, K. Freese, N. R. Shah and B. Shakya, Phys. Rev. D **95** (2017) no.11, 115036 [arXiv:1703.07800 [hep-ph]].
- [21] U. Ellwanger and M. Rodriguez-Vazquez, JHEP **11** (2017), 008 [arXiv:1707.08522 [hep-ph]].
- [22] S. Baum, M. Carena, N. R. Shah and C. E. M. Wagner, JHEP **04** (2018), 069 [arXiv:1712.09873 [hep-ph]].
- [23] P. Basler, S. Dawson, C. Englert and M. Mühlleitner, Phys. Rev. D **99** (2019) no.5, 055048 [arXiv:1812.03542 [hep-ph]].
- [24] S. Baum, N. R. Shah and K. Freese, JHEP **04** (2019), 011 [arXiv:1901.02332 [hep-ph]].
- [25] D. Barducci, K. Mimasu, J. M. No, C. Vernieri and J. Zurita, JHEP **02** (2020), 002 [arXiv:1910.08574 [hep-ph]].
- [26] T. Biekötter, A. Grohsjean, S. Heinemeyer, C. Schwanenberger and G. Weiglein, Eur. Phys. J. C **82** (2022) no.2, 178 [arXiv:2109.01128 [hep-ph]].
- [27] H. Abouabid, A. Arhrib, D. Azevedo, J. E. Falaki, P. M. Ferreira, M. Mühlleitner and R. Santos, JHEP **09** (2022), 011 [arXiv:2112.12515 [hep-ph]].
- [28] A. M. Sirunyan *et al.* [CMS], JHEP **03**, 055 (2020) doi:10.1007/JHEP03(2020)055 [arXiv:1911.03781 [hep-ex]].
- [29] G. Aad *et al.* [ATLAS], Eur. Phys. J. C **81**, no.5, 396 (2021) doi:10.1140/epjc/s10052-021-09117-5 [arXiv:2011.05639 [hep-ex]].
- [30] A. Tumasyan *et al.* [CMS], “Search for a new resonance decaying into two spin-0 bosons in a final state with two photons and two bottom quarks in proton-proton collisions at $\sqrt{s} = 13$ TeV,” [arXiv:2310.01643 [hep-ex]].
- [31] A. Tumasyan *et al.* [CMS], “Search for a heavy Higgs boson decaying into two lighter Higgs bosons in the $\tau\tau b\bar{b}$ final state at 13 TeV,” JHEP **11** (2021), 057 [arXiv:2106.10361 [hep-ex]].
- [32] A. Tumasyan *et al.* [CMS], Phys. Lett. B **842** (2023), 137392 [arXiv:2204.12413 [hep-ex]].
- [33] G. Aad *et al.* [ATLAS], JHEP **10** (2023), 009 [arXiv:2307.11120 [hep-ex]].